Pump Geometries

Since the task specifications for a pump (or turbine or compressor or other machine) can be reduced to the single parameter, N_D, it is not surprising that the overall or global geometries of pumps, that have evolved over many decades, can be seen to fit quite neatly into a single parameter family of shapes. This family is depicted in figure 1. These geometries reflect the fact that an axial flow machine, whether a pump, turbine, or compressor, is more efficient at high specific speeds (high flow rate, low head) while a radial machine, that uses the centrifugal effect, is more efficient at low specific speeds (low flow rate, high head).
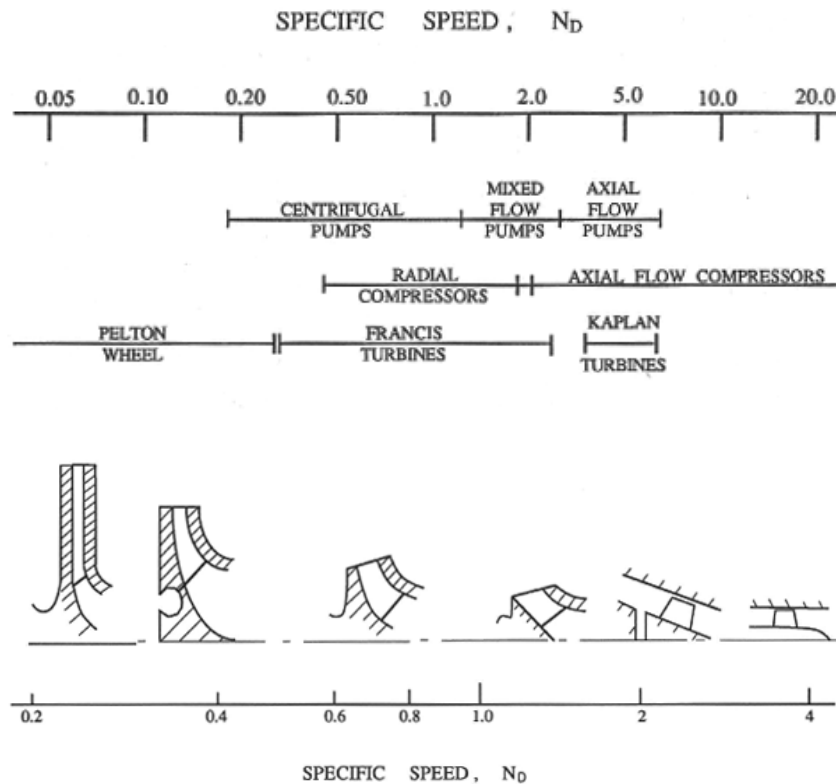

Figure 1: Typical turbomachine geometries for a range of specific speeds (from Sabersky, Acosta and Hauptmann 1989).

Examples of what different pumps look like are shown in Figures 2 and 4. A typical centrifugal pump is shown in Figure 2 and consists of two key parts that need careful detailed design, namely the rotating element or **impeller** and the **volute** that collects the flow exiting the impeller and guides it into the discharge pipe with the minimum of hydraulic loss. In fact, much of the hydraulic loss within the pump does, in fact occur within the volute since the flow is usually decelerating as it is collected and channelled. In this respect the design of the volute and the cutwater is an important aspect of centrifugal pump design. Volutes exhibit a range of different designs, some with two separate, diametrically-opposed collectors (a double volute with two cutwaters) and some with guide vanes.

A typical non-cavitating performance characteristic for a centrifugal pump is shown in figure 3 for the Impeller X/Volute A combination (Chamieh 1983) described in section (Mbbi). The design flow coefficient
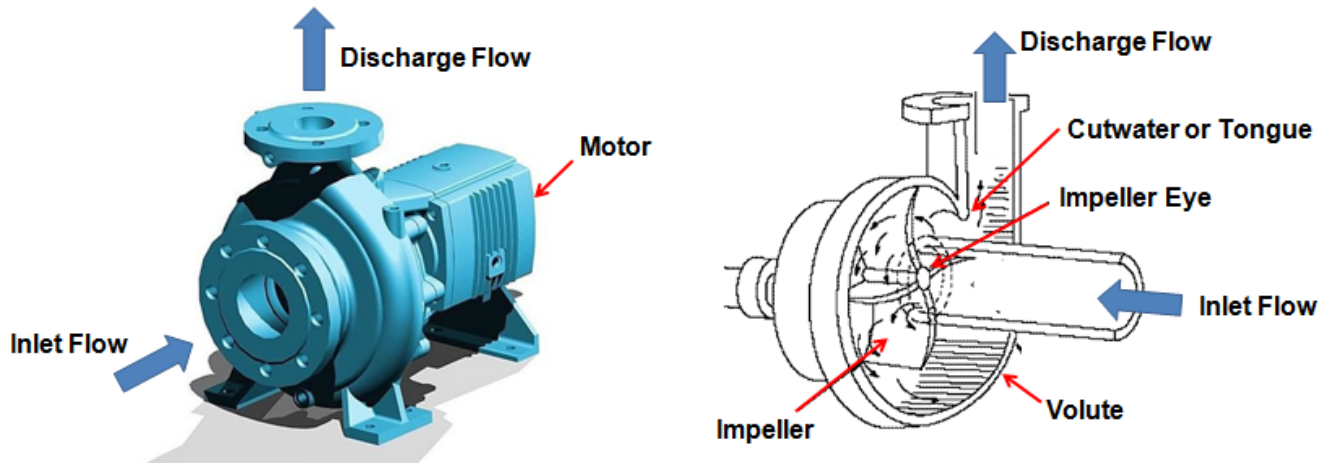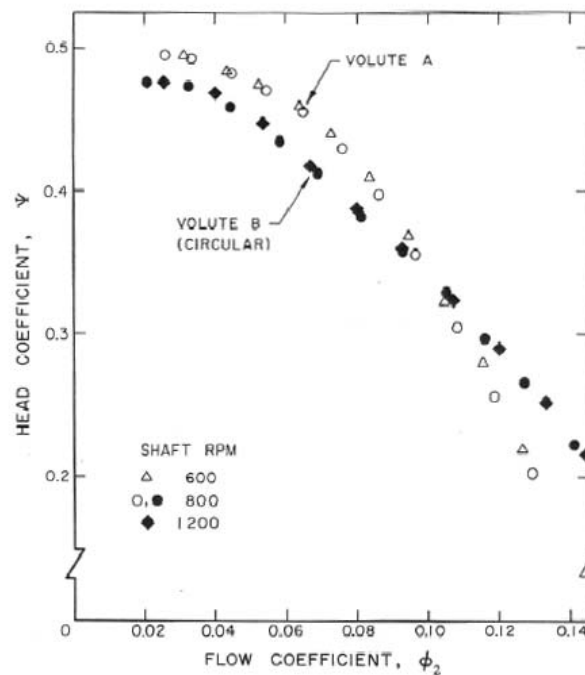
Figure 2: Examples of centrifugal pumps.

Figure 3: Typical non-cavitating performance for a centrifugal pump, namely Impeller X (see section (Mbbi)) with Volute A and a circular volute of uniform cross-section (from Chamieh 1983).

for this pump is $\phi_2 = 0.092$ but we note that it performs reasonably well down to about 30% of this design flow. This flexibility is characteristic of centrifugal pumps. Data is presented for three different shaft speeds, namely 600, 800 and $1200 rpm$; since these agree closely we can conclude that there is no perceptible effect of Reynolds number for this range of speeds. The effect of a different volute is also illustrated by the data for Volute B which is a circular volute of circumferentially uniform area. In theory this circular volute is not well matched to the impeller discharge flow and the result is that, over most of the range of flow coefficient, the hydraulic performance is inferior to that with Volute A. However, Volute B is superior at high flow coefficients. This suggests that the flow in Volute A may be more pathological than one would like at these high flow coefficients (see sections (Mbdd) and (Mbde)). It further serves to emphasize the importance of a volute (or diffuser) and the need for an understanding of the flow in a volute at both design and off-design conditions.

Examples of an axial flow pump and a mixed flow pump (the semantics for a design at intermediate specific speeds) are shown in Figure 4. An axial flow pump is very similar to a ducted propeller though the treatment of the impeller tip and the tip clearance flow can differ significantly from one application to another. Sometimes a set of stator vanes is included in order to recover the dynamic head from the swirling flow that exits the impeller as shown in the mixed flow pump diagram. As with the centrifugal pump volute, substantial hydraulic losses can occur unless the stator is carefully designed, especially when the cross-sectional area is increasing through the stator as is the case on the left of Figure 4. Another factor that often enters the design is the need to provide bearing support close to the impeller and the stator vanes are frequently used for this purpose also.
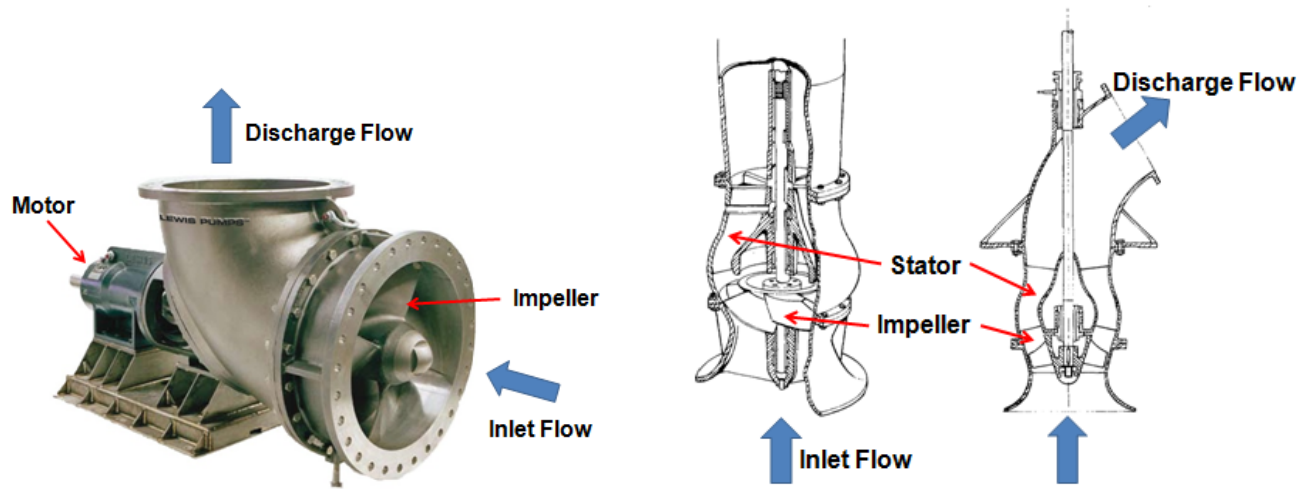

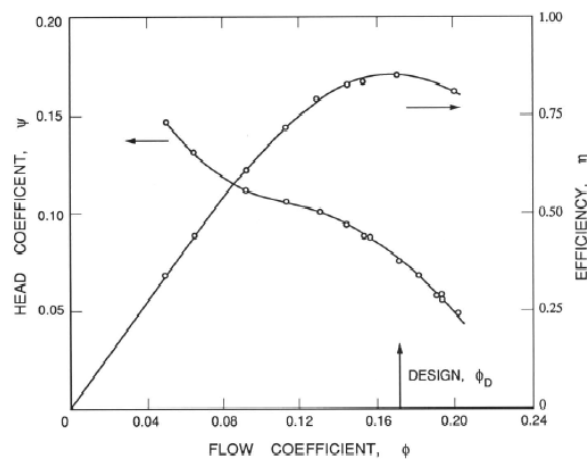
Figure 4: Examples of axial and mixed flow pumps.

Figure 5: Typical non-cavitating performance characteristics for a $20.3cm$ diameter, 3-bladed axial flow pump with a hub-tip ratio, R_H/R_T, of 0.45 running at about $1500rpm$. At the blade tip the chord is $7.3cm$, the solidity is 0.344 and the blade angle, β_{bT}, is 11.9°. Adapted from Guinard $et~al.$ (1953).

Examples of the non-cavitating performance of axial and mixed flow pumps are shown in Figures 5, 6, 7 and 8. Typical non-cavitating performance characteristics of a Peerless axial flow pump are shown in figure 5. This unshrouded pump has a design flow coefficient $\phi_2 = 0.171$. The maximum efficiency at this design point is about 85%. Axial flow pumps are more susceptible to flow separation and stall than centrifugal pumps and could therefore be considered less versatile. The depression in the head curve of figure 5 in
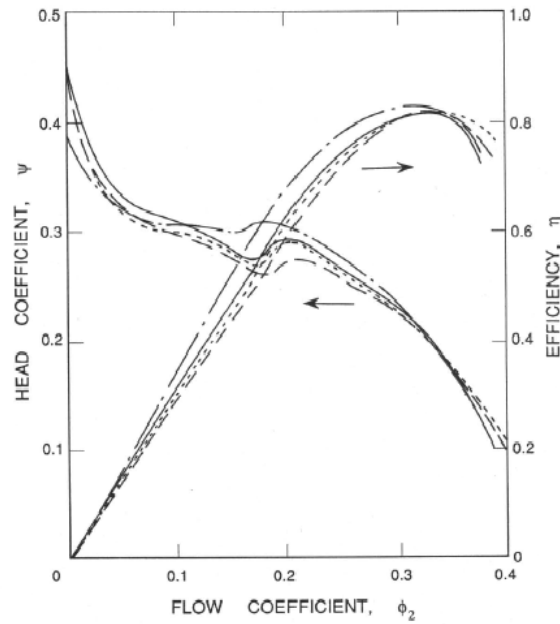
Figure 6: Typical non-cavitating performance characteristics for a four-bladed axial flow pump with tip blade angle, β_{bT}, of about 18°, a hub-tip ratio, R_H/R_T, of 0.483, a solidity of 0.68 and four different blade profiles (yielding the set of four performance curves). Adapted from Oshima and Kawaguchi (1963).
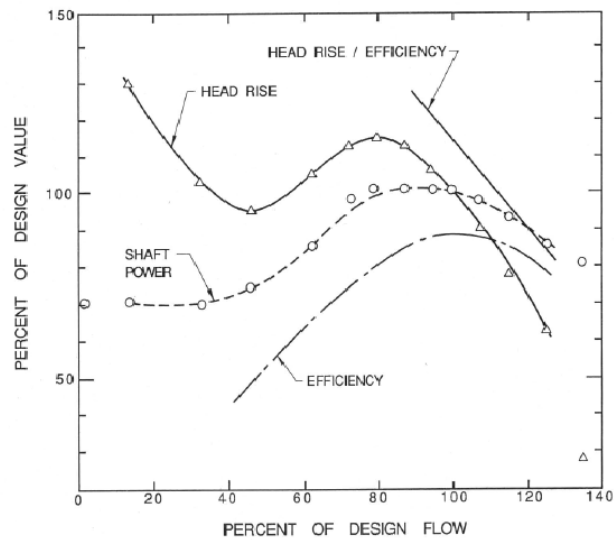

Figure 7: Characteristics of a mixed flow pump (Myles 1966).

the range $\phi_2 = 0.08 \rightarrow 0.12$ is indicative of flow separation and this region of the head/flow curve can therefore be quite sensitive to the details of the blade profile since small surface irregularities can often have a substantial effect on separation. This is illustrated by the data of figure 6 which presents the non-cavitating characteristics for four similar axial flow pumps with slightly different blade profiles. The kinks in the curves are more marked in this case and differ significantly from one profile to another. Note also that there are small regions of positive slope in the head characteristics. This often leads to instability and to fluctuating pressures and flow rates through the excitation of the surge and stall mechanisms discussed in the following chapters. Sometimes the region of positive slope in the head characteristic can be even more marked as in the example presented in figure 7 in which the stall occurs at about 80% of the design flow. As a final example of non-cavitating performance we include in figure 8, the effect of the blade angle
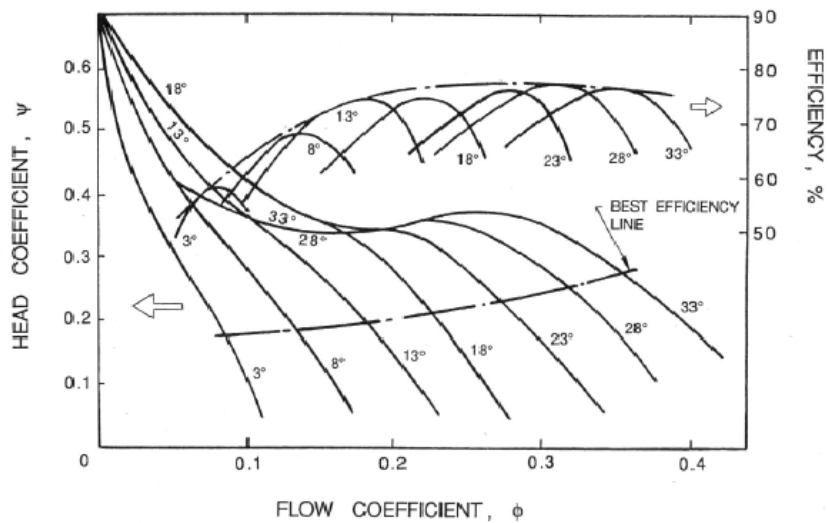
Figure 8: Head and efficiency characteristics for an axial flow pump with different tip blade angles, β_{bT} (from Peck 1966).

in an axial flow pump; note that angles of the order of 20° to 30° seem to be optimal for many purposes.

**

The same basic family of pump geometries is presented quantitatively in figure 9, where the anticipated head and flow coefficients are also plotted. The existence of this parametric family of designs has emerged almost exclusively as a result of trial and error though modern analyses have revealed the fluid mechanical reasons for these optima.

Normally, turbomachines are designed to have their maximum efficiency at the design specific speed, N_D. Thus, in any graph of efficiency against specific speed, each pump geometry will trace out a curve with a maximum at its optimum specific speed, as illustrated by the individual curves in figure 10. Furthermore, Balje (1981) has made note of another interesting feature of this family of curves in the graph of efficiency against specific speed. First, he corrects the curves for the different viscous effects which can occur in machines of different size and speed, by comparing the data on efficiency at the same effective Reynolds number using the diagram reproduced as figure 11. Then, as can be seen in figure 10, the family of curves for the efficiency of different types of machines has an upper envelope with a maximum at a specific speed of unity. Maximum possible efficiencies decline for values of N_D greater or less than unity. Thus the "ideal" pump would seem to be that with a design specific speed of unity, and the maximum obtainable efficiency seems to be greatest at this specific speed. Fortunately, from a design point of view, one of the specifications has some flexibility, namely the shaft speed, Ω. Though the desired flow rate and head rise are usually fixed, it may be possible to choose the drive motor to turn at a speed, Ω, which brings the design specific speed close to the optimum value of unity.
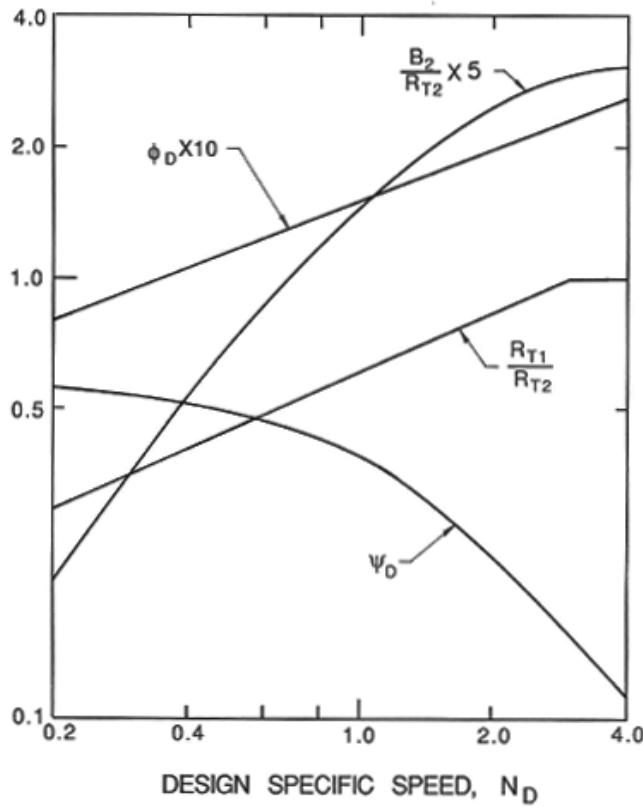
Figure 9: General design guidelines for pumps indicating the optimum ratio of inlet to discharge tip radius, R_{T1}/R_{T2}, and discharge width ratio, B_2/R_{T2}, for various design specific speeds, N_D. Also shown are approximate pump performance parameters, the design flow coefficient, ϕ_D, and the design head coefficient, ψ_D (adapted from Sabersky, Acosta and Hauptmann 1989).
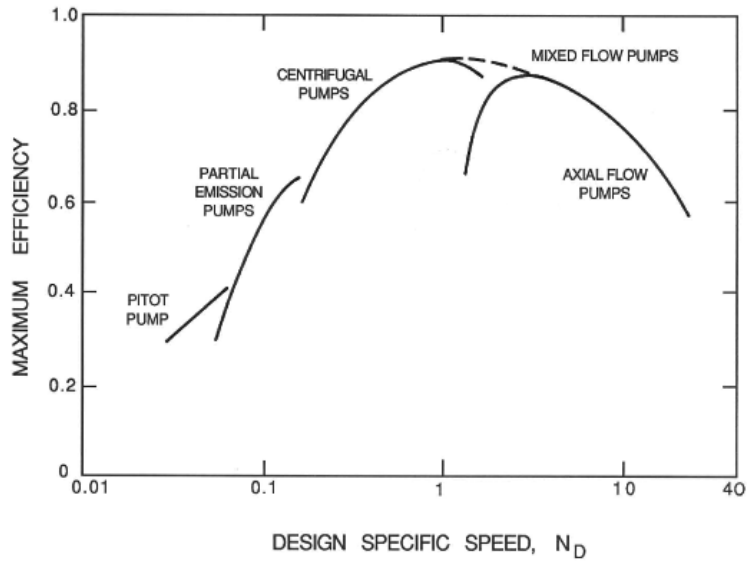

Figure 10: Compilation by Balje (1981) of maximum efficiencies for various kinds of pumps as a function of design specific speed, N_D. Since efficiency is also a function of Reynolds number the data has been corrected to a Reynolds number, $2\Omega R_{T2}^2/\nu$, of 10^8.

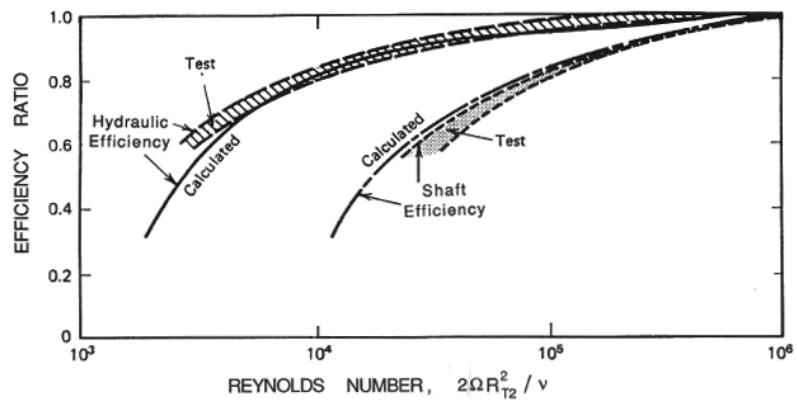Figure 11: The dependence of hydraulic efficiency, η_P, and shaft efficiency, η_S, on Reynolds number, $2\Omega R_{T2}^2/\nu$ (from Balje 1981).